

Higgs boson decays to four fermions through an abelian hidden sector

Shrihari Gopalakrishna^a, Sunghoon Jung^b, and James D. Wells^{c,b}^a Physics Department, Brookhaven National Laboratory, Upton, NY 11973^b MCTP, University of Michigan, Ann Arbor, MI 48109^c CERN, Theory Division (PH-TH), CH-1211 Geneva 23, Switzerland

We consider a generic abelian hidden sector that couples to the Standard Model only through gauge-invariant renormalizable operators. This allows the exotic Higgs boson to mix with the Standard Model Higgs boson, and the exotic abelian gauge boson to mix with the Standard Model hypercharge gauge boson. One immediate consequence of spontaneous breaking of the hidden sector gauge group is the possible decay of the lightest Higgs boson into four fermions through intermediate exotic gauge bosons. We study the implications of this decay for Higgs boson phenomenology at the Fermilab Tevatron Collider and the CERN Large Hadron Collider. Our emphasis is on the four lepton final state.

PACS numbers:

Introduction. The fundamental theory may be significantly richer than the Standard Model (SM) world that we have directly probed. Copies of many other gauge theories may be inaccessible to us because the particles that form our bodies are not charged under them. Is there a method to explore such hidden worlds given the limited collection of charges that we can directly probe? The answer is not assured, but an opportunity can be identified [1, 2, 3, 4, 5].

The SM has two gauge invariant, flavor-neutral operators that are relevant (dimension < 4): the hypercharge field-strength tensor $B_{\mu\nu}$ and the SM Higgs mass operator $j_{SM} \hat{H}^\dagger \hat{H}$. Hidden sector (i.e., non-SM states with no SM charge) abelian gauge bosons X and Higgs bosons H can couple to these operators in a gauge invariant, renormalizable manner [27]:

$$X_{\mu\nu} B^{\mu\nu}; \text{ and } j_H \hat{H}^\dagger \hat{H} j_{SM} \hat{H}^\dagger \hat{H}; \quad (1)$$

These couplings give us the opportunity we are looking for to see the effects of a hidden sector by virtue of their interactions with states we can observe.

In this letter we investigate the implications for Higgs boson phenomenology of the simultaneous existence of the two operators in Eq. (1). We do not tie ourselves to any particular model of the hidden abelian sector. We note that if the kinetic mixing between the gauge bosons is large, precision electroweak and dedicated collider searches may see the effects [4, 6, 7, 8, 9]. For our purposes, we only need the kinetic mixing to be non-zero and large enough to allow prompt decays of the exotic gauge boson eigenstate. We also note that the pure mixing effects of H and H_{SM} can be probed well by colliders [1, 2, 10, 11, 12] even if no exotic decay modes are kinematically accessible. However, it would be more difficult in that circumstance to know what the origin is of the shift in Higgs boson phenomenology at colliders. For related discussion on the phenomenology of a hidden sector see Ref. [13].

Instead, what we focus on here is the prospect of the exotic gauge boson being sufficiently light such that the lightest Higgs boson decays into a pair of them [14]. The

decay of the Higgs boson into two X bosons is through Higgs boson mixing. The X boson will then decay into SM fermions if there is even a tiny amount of kinetic mixing, which we assume to be the case. The X bosons could have competing branching fraction into other exotic states potentially leading to invisible decays or even more background-free topologies than considered here. We neglect these possibilities in order to keep our analysis simple and our assumptions to a minimum. We are particularly interested in leptonic final states. Thus, the subject of this paper is to provide the details of how $h \rightarrow X X \rightarrow \ell\ell\ell\ell$ is possible within this theoretical framework, and to explore the detectability of this channel at the Fermilab Tevatron and CERN LHC.

Theory framework. We consider an extra $U(1)_X$ factor in addition to the SM gauge group. The only coupling of this new gauge sector to the SM is through kinetic mixing with the hypercharge gauge boson B . The kinetic energy terms of the $U(1)_X$ gauge group are

$$L_X^{KE} = \frac{1}{4} \hat{X}^\dagger \hat{X} + \frac{1}{2} \hat{X}^\dagger \hat{B}; \quad (2)$$

where we take the parameter χ to be consistent with precision electroweak constraints. Hats on fields imply that gauge fields do not have canonically normalized kinetic terms.

As an example, we note that heavy states that are charged under both $U(1)_Y$ and $U(1)_X$ can typically induce a χ at the loop level [15] given by $g^0 g_X = (16\pi^2)^{-1} 10^3$. Tree-level mixing, although possible, will be absent if the $U(1)_X$ is the remnant of a spontaneously broken non-abelian gauge symmetry. If the scale of $U(1)_X$ breaking is not too far above the electroweak scale, a radiatively generated χ will be quite small. We take the $U(1)_X$ breaking VEV ~ 1 TeV.

We introduce a new Higgs boson H in addition to the usual SM Higgs boson H_{SM} . Under $SU(2)_L \times U(1)_Y \times U(1)_X$ we take the representations $H_{SM} : (2; 1/2; 0)$ and $H : (1; 0; q_X)$, with q_X arbitrary. The Higgs sector La-

Lagrangian is

$$L = \mathcal{D}_{SM} \bar{f} \mathcal{D}_{SM} f + \mathcal{D}_H \bar{f} \mathcal{D}_H f + m_H^2 \bar{f} f + m_{SM}^2 \bar{f} f \quad (3)$$

so that $U(1)_X$ is broken spontaneously by $\langle h_H \rangle = \frac{v}{\sqrt{2}}$, and electroweak symmetry is broken spontaneously as usual by $\langle h_{SM} \rangle = (0; v/\sqrt{2})$.

One can diagonalize the kinetic terms by redefining $\hat{X}; \hat{B} \rightarrow X; B$ with

$$\begin{pmatrix} X \\ B \end{pmatrix} = \begin{pmatrix} \cos \theta & \sin \theta \\ -\sin \theta & \cos \theta \end{pmatrix} \begin{pmatrix} \hat{X} \\ \hat{B} \end{pmatrix}$$

The covariant derivative is then

$$D = \partial + i(g_X Q_X + g^0 Q_Y)X + ig^0 Q_Y B + igT^3 W^3 \quad (4)$$

where $\frac{g^0}{g} = \frac{v}{\sqrt{2}}$.

After a $GL(2; R)$ rotation to diagonalize the kinetic terms followed by an $O(3)$ rotation to diagonalize the 3×3 neutral gauge boson mass matrix, we can write the mass eigenstates as (with $s_x = \sin x, c_x = \cos x$)

$$\begin{pmatrix} B \\ W^3 \\ X \end{pmatrix} = \begin{pmatrix} c_W & s_W c & 0 \\ s_W c & c_W c & 0 \\ 0 & s & c \end{pmatrix} \begin{pmatrix} A \\ Z \\ Z^0 \end{pmatrix} \quad (5)$$

where the usual weak mixing angle and the new gauge boson mixing angle are

$$s_W = \frac{g^0}{\sqrt{g^2 + g^{02}}}; \quad \tan(2\theta) = \frac{2s_W}{1 - \frac{g^0}{g}} \quad (6)$$

with $z = M_X^2/M_{Z^0}^2, M_X^2 = 2g_X^2 c_X^2, M_{Z^0}^2 = (g^2 + g^{02})v^2/4$. M_{Z^0} and M_X are masses before mixing. The photon is massless (i.e., $M_A = 0$), and the two heavier gauge boson mass eigenvalues are

$$M_{Z,Z^0} = \frac{M_{Z^0}^2}{2} \left[1 + s_W^2 z + \frac{z}{q} \sqrt{(1 - s_W^2 z)^2 + 4s_W^2 z} \right] \quad (7)$$

valid for $z < (1 - s_W^2)^2$ ($Z \neq Z^0$ otherwise). Since we assume that $z \ll 1$, mass eigenvalues are taken as $M_Z = M_{Z^0} = 91.19$ GeV and $M_{Z^0} = M_X$.

The two real physical Higgs bosons h_{SM} and h_H mix after symmetry breaking, and the mass eigenstates $h; H$ are

$$\begin{pmatrix} h_{SM} \\ h_H \end{pmatrix} = \begin{pmatrix} c_h & s_h \\ -s_h & c_h \end{pmatrix} \begin{pmatrix} h \\ H \end{pmatrix} \quad (8)$$

The mixing angle and mass eigenvalues are

$$\tan(2\theta_h) = \frac{v}{2\sqrt{2}} \quad (8)$$

$$M_{h,H}^2 = \frac{v^2}{2} \left[1 \pm \sqrt{1 + \frac{2}{z}} \right] \quad (9)$$

Although the mixing angle depends on the many unknown parameters of Eq.(3), we will treat the resulting h as an input along with the Higgs boson masses.

Now we are able to present the couplings of the Z^0 to various SM states.

Fermion couplings: Couplings to SM fermions are

$$\begin{aligned} Z &: \frac{ig}{c_W} [c(1 - s_W t)] T_L^3 \frac{(1 - t = s_W)}{(1 - s_W t)} S_W^2 Q \\ Z^0 &: \frac{ig}{c_W} [c(t + s_W)] T_L^3 \frac{(t + = s_W)}{(t + s_W)} S_W^2 Q \end{aligned} \quad (10)$$

where we have used $Q = T_L^3 + Q_Y$ and $t = s/c$. The photon coupling is as in the SM and is not shifted.

Triple gauge boson couplings: Denoting the coupling relative to the corresponding SM coupling as R , we find $R_{AW+W} = 1, R_{ZW+W} = c$ and $R_{Z^0W+W} = s$ (the last is compared to the SM $ZW+W$ coupling). In our case, to leading order we have $c \approx 1, s \approx 1$.

Higgs couplings: The Higgs couplings are

$$\begin{aligned} hff &: ig \frac{m_f}{v}; \quad hWW : 2ic_h \frac{M_W^2}{v} \\ hZZ &: 2ic_h \frac{M_{Z^0}^2}{v} (c + s_W s)^2 - 2is_h \frac{M_X^2}{v} s^2; \\ hZ^0 Z^0 &: 2ic_h \frac{M_{Z^0}^2}{v} (s + s_W c)^2 - 2is_h \frac{M_X^2}{v} c^2; \quad (11) \\ hZ^0 Z &: 2ic_h \frac{M_{Z^0}^2}{v} (c + s_W s)(s + s_W c) \\ &: 2is_h \frac{M_X^2}{v} s c; \end{aligned}$$

Parameters and Precision Electroweak Constraints. Electroweak precision observables such as M_W, z and A_{LR} constrain the theory. These constraints have been discussed in greater detail in Refs. [4, 6, 7, 8, 9]. For our theory, given the experimental accuracy [16] of precision electroweak observables including those mentioned above, we find the constraint

$$\frac{v}{M_{Z^0} = M_Z} \cdot 10^{-2} \quad (12)$$

This is expected given that the fractional accuracy of EW precision measurements are at the 10^{-4} level, and in our model the deviations appear at $O(z^2)$.

Fits to electroweak precision observables [17] constrain the SM Higgs mass to be $\log(M_{Higgs} = 1 \text{ GeV}) = 1.93^{+0.16}_{-0.17}$. This can be turned into a constraint on our model by noting that all couplings to SM fields involving h have an additional factor of c_h while those for H have s_h , which results in

$$c_h^2 \log \frac{M_h}{1 \text{ GeV}} + s_h^2 \log \frac{M_H}{1 \text{ GeV}} \approx 1.93^{+0.16}_{-0.17} \quad (13)$$

Equivalently, one can state the constraints in terms of the S and T parameters, following the discussion in Ref. [18].

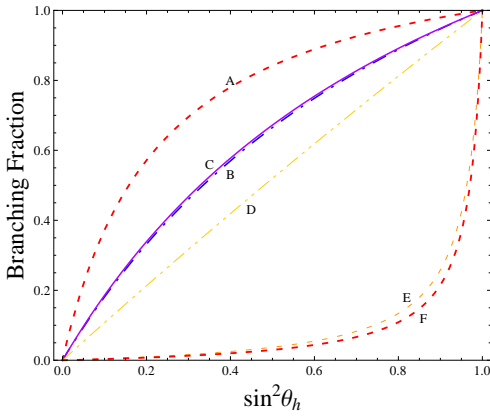


FIG. 1: Branching ratio of $h \rightarrow Z^0 Z^0$ as a function of $\sin^2 \theta_h$ for various M_{Z^0} and M_h , with $\tan \beta = 10^4$. Benchmark points are shown in Table I.

Since we do not specify the value of the heavier Higgs mass, we have the freedom to choose it such that there is no difficulty with precision electroweak constraints. Even if we choose a much heavier Higgs boson for our second eigenstate, there are well-known ways the theory can be augmented to be compatible with the data [18].

Decay Branching Fractions. We now turn to the actual decay branching fractions of the Higgs boson and Z^0 mass eigenstate. We are particularly interested in the frequency of $h \rightarrow Z^0 Z^0$ and the leptonic branching fractions of Z^0 .

$h \rightarrow Z^0 Z^0$ decay: In Fig. 1 we show the $h \rightarrow Z^0 Z^0$ branching ratio as a function of $\sin^2 \theta_h$, computed using HDECAY [19]. A 120 GeV (250 GeV) Higgs boson has total width of 10 MeV (2.1 GeV) when $M_{Z^0} = 5$ GeV and $c_h^2 = 0.5$. We do not include any heavy exotic states that the X couples to, which would require either considering the additional invisible decay modes, studied well elsewhere, or much more spectacular and model-dependent decay chains to SM particles.

Z^0 decay: The Z^0 coupling to the SM sector is proportional to the tiny ϵ , making the width rather small, but these are the only modes kinematically allowed for the Z^0 to decay into. The Z^0 total width for $\tan \beta = 10^4$ is $5.8 \cdot 10^{10}$, $2.7 \cdot 10^9$, $8.2 \cdot 10^9$ and $2.0 \cdot 10^7$ GeV for $M_{Z^0} = 5, 20, 50$ and 100 GeV respectively. This decay width is too small to be resolved by LHC experiment, but large enough to yield prompt decays. The total width for any other Z^0 can be obtained by scaling the above width by ϵ^2 . Displaced vertices begin to be allowed when $\epsilon < 10^{-5}$, which would be another interesting sign of exotic physics in the Higgs boson decays. In Fig. 2 we show the Z^0 branching ratio into two body final states as a function of M_{Z^0} .

Four Lepton Modes at the Tevatron and LHC. We focus on the mode $h \rightarrow Z^0 Z^0 \rightarrow 4\ell$ in our analysis with $\ell = e, \mu$. In presenting results in this section, we will choose $\tan \beta = 10^4$, $\sqrt{s} = 1$ TeV, and unless mentioned oth-

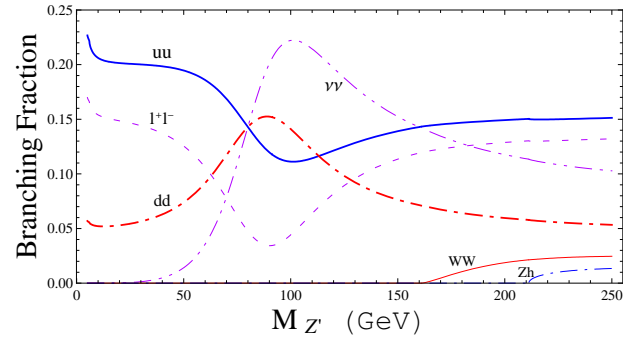


FIG. 2: Branching ratio of Z^0 into two body final states as a function of M_{Z^0} with $c_h^2 = 0.5$ and $\tan \beta = 10^4$.

| Point | A | B | C | D | E | F |
|------------------------|--------|---------|--------|---------|--------|---------|
| (M_h, M_{Z^0}) (GeV) | 120, 5 | 120, 50 | 150, 5 | 150, 50 | 250, 5 | 250, 50 |

TABLE I: Six benchmark points that we study.

erwise, take $c_h^2 = 0.5$. For illustration, we choose six benchmark points as shown in Table I for which we compute the differential distributions, make cuts and find the significance at the Tevatron and LHC. We make use of the narrow width approximation and analyze in succession: $pp \rightarrow h \rightarrow Z^0 Z^0$ followed by $Z^0 \rightarrow 4\ell$.

The gluon fusion process $gg \rightarrow h$ is the largest production channel at the Tevatron ($\sqrt{s} = 1.96$ TeV) and the LHC ($\sqrt{s} = 14$ TeV). For instance, at the Tevatron, NLO ($gg \rightarrow h$) = 0.85 pb for $M_h = 120$ GeV while the sum of the other channels gives 0.33 pb; the corresponding cross-sections at the LHC are 40.25 pb and 7.7 pb respectively [20, 21]. We include only gluon fusion computed at NLO using HIGLU [20].

The main sources of background are the SM processes $pp \rightarrow h \rightarrow ZZ \rightarrow 4\ell$, and $pp \rightarrow VV \rightarrow 4\ell$ where VV denotes $ZZ, \gamma\gamma$ and $Z\gamma$ channels. The $pp \rightarrow t$ production cross-section is large and 4-lepton events from this process can be a source of (reducible) background at the LHC, but we take it that this can be adequately suppressed (for details see Ref. [22]).

We use MadGraph [23] to obtain all matrix elements, and generate event samples using MadEvent [24] with CTEQ6L1 PDF [25]. The cross-sections for the process $pp \rightarrow h \rightarrow Z^0 Z^0 \rightarrow 4\ell$ at the LHC without any cuts are shown in Fig. 3, and the corresponding ones at the Tevatron while similar in shape, are smaller by about 50, and will be discussed later in this section. We present the ee channels here, but this can be extended to include $4e$ and 4μ channels. The cross-section approaches zero as $c_h^2 \rightarrow 1$ because h will not couple to the X boson, and also as $c_h^2 \rightarrow 0$ because h does not couple to the gluon in this limit. In these limits our analysis can be applied to probe the second Higgs mass eigenstate H .

To help in distinguishing signal from background, we make various kinematical cuts. We pair two opposite sign

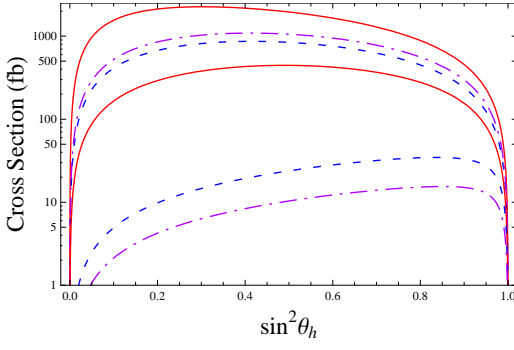


FIG. 3: Total cross section of the process $pp \rightarrow h \rightarrow Z^0 Z^0 \rightarrow 4l$ at LHC as a function of $\sin^2 \theta_h$. From top to bottom, lines correspond to points A, C, B, D, E, F. No cuts have been applied.

leptons with $R_{\ell\ell} < 2.5$ to ensure that they come from the same Z^0 , and for this pair, from the dilepton invariant mass $M_{\ell\ell}$. We also form the 4-lepton invariant mass $M_{\ell\ell\ell\ell}$. In Fig. 4, we show 4-lepton invariant mass plots for point A at LHC and point F at Tevatron, for reference.

Based on the differential distributions, we impose the following cuts in order to maximize signal over background:

$$\begin{aligned}
 \text{Basic cuts: } & p_T, > 20; 10; 10; 10 \text{ GeV}; \quad |j \cdot j| < 2.5; \\
 R \text{ cut: } & 0.05 < R_{\ell\ell} < 2.5; \\
 M_{ij} \text{ cuts: } & M_{ee} = M_{\mu\mu} > 10 \text{ GeV}; \\
 M_{ijkl} \text{ cut: } & M_{ee} = M_{\mu\mu} > M_h - 10 \text{ GeV} \quad : \quad (14)
 \end{aligned}$$

The four-lepton cut around M_h is achieved by hypothesizing a Higgs boson resonance and scanning across that hypothesis. Such a scan is realizable in our case since the signal stands clearly above the continuum background. The signal and background cross-sections are shown in Table II. We find that the 4-lepton invariant mass cut is most effective in reducing the background. The $S=B$ is good for all the benchmark points, but can be improved further by the additional cut: $M_{\ell\ell} \notin M_Z - 10 \text{ GeV}$, which removes on-shell Z -bosons surviving in the data sample.

Conclusions. In our chosen example cases with large mixing among the SM and hidden sector Higgs bosons and light-enough M_{Z^0} for $h \rightarrow Z^0 Z^0$ to be on-shell, the prospects for seeing the signal at the LHC are excellent. The signals for the various examples are well above background after all cuts have been applied. The Tevatron is also beginning to achieve the sensitivity required to see the signal; however, there the key challenge is not signal to background, but overall signal rate and luminosity to collect enough events to reconstruct a resonance. Once sufficient luminosity is achieved, and after more tailored techniques are applied to the problem, such as those to search for SM ZZ events [26], the Tevatron should be in a position to probe well a light Higgs boson decaying in

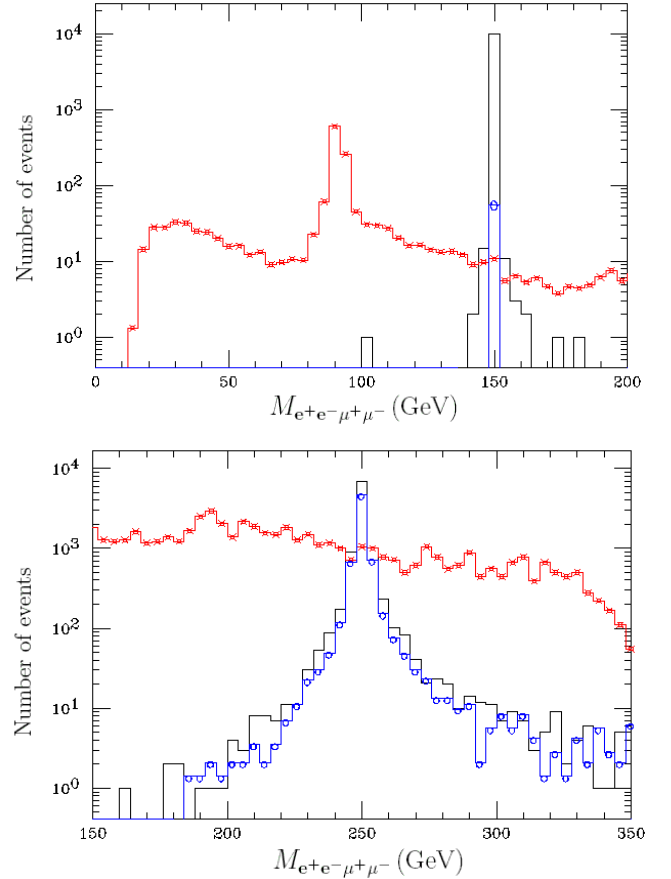


FIG. 4: $M_{e^+e^- \mu^+\mu^-}$ (in GeV) versus number of events (arbitrary luminosity) for benchmark point D at the Tevatron (top), and point F at the LHC (bottom). No cuts are applied yet. Black solid line represents $h \rightarrow ZZ \rightarrow 4l$ signal, red crossed $ZZ \rightarrow 4l$, and blue circled $h \rightarrow ZZ \rightarrow 4l$.

| Tevatron | A | B | C | D | E | F |
|-------------|----------|-----------|----------|-----------|------------|------------|
| $Z^0 Z^0$ | 8.8; 4.3 | 3.9; 0.8 | 4.2; 2.4 | 2.3; 0.8 | 0.05; 0.02 | 0.03; 0.01 |
| $hZ Z$ (ab) | 0.8; 0 | 1.4; 0 | 7.4; 0 | 12.8; 0 | 17; 1.6 | 21.4; 1.8 |
| VV | 9.7; 4.3 | 10^{-3} | 9.7; 3.5 | 10^{-3} | 9.7; 0.01 | |
| LHC | A | B | C | D | E | F |
| $Z^0 Z^0$ | 631; 245 | 236; 44 | 348; 173 | 212; 57 | 12; 5.6 | 6.5; 2.2 |
| $hZ Z$ (ab) | 0; 0 | 130; 1.2 | 630; 2.3 | 1280; 2.5 | 3440; 850 | 4840; 846 |
| VV | 67; 0.02 | | 67; 0.03 | | 67; 0.3 | |

TABLE II: Signal and background cross-sections in fb (only $hZ Z$ in ab) for the Tevatron and LHC in the form: (basic cuts, all cuts). "Basic cuts" refers only to the p_T and η cuts in the first line of Eq. 14. VV denotes the contributions from ZZ , and Z . K-factors have not been included.

the manner proposed here.

Acknowledgments. We are grateful to S. Protopopescu, J. Qian and M. Strassler for discussions, and J. Allwall and R. Frederix for generous technical help. This work is supported in part by the DOE. SG is supported in part

by the DOE grant DE-AC02-98CH10886 (BNL). SJ is supported in part by Samsung Scholarship.

-
- [1] R. Schabinger and J. D. Wells, *Phys. Rev. D* **72**, 093007 (2005) [arXiv:hep-ph/0509209].
- [2] M. J. Strassler and K. M. Zurek, *Phys. Lett. B* **651**, 374 (2007) [arXiv:hep-ph/0604261].
- [3] B. Patt and F. Wilczek, arXiv:hep-ph/0605188.
- [4] J. Kumar and J. D. Wells, *Phys. Rev. D* **74**, 115017 (2006) [arXiv:hep-ph/0606183].
- [5] J. March-Russell, S. M. West, D. Cumberbatch and D. Hooper, arXiv:0801.3440.
- [6] K. S. Babu, C. F. Kolda and J. March-Russell, *Phys. Rev. D* **57**, 6788 (1998) [arXiv:hep-ph/9710441].
- [7] W. F. Chang, J. N. Ng and J. M. S. Wu, *Phys. Rev. D* **74**, 095005 (2006) [arXiv:hep-ph/0608068] and *Phys. Rev. D* **75**, 115016 (2007) [arXiv:hep-ph/0701254].
- [8] T. G. Rizzo, arXiv:hep-ph/0610104.
- [9] P. Langacker, arXiv:0801.1345 [hep-ph].
- [10] R. Barbieri, T. Gregoire and L. J. Hall, arXiv:hep-ph/0509242.
- [11] Z. Chacko, Y. Nomura, M. Papucci and G. Perez, *JHEP* **0601**, 126 (2006) [arXiv:hep-ph/0510273].
- [12] M. Bowen, Y. Cui and J. D. Wells, *JHEP* **0703**, 036 (2007) [arXiv:hep-ph/0701035].
- [13] R. Foot, H. Lew and R. R. Volkas, *Phys. Lett. B* **272**, 67 (1991); K. S. Babu and G. Seidl, *Phys. Rev. D* **70**, 113014 (2004) [arXiv:hep-ph/0405197]; R. Foot and X. G. He, *Phys. Lett. B* **267**, 509 (1991).
- [14] Higgs has been noted in a related context by M. J. Strassler, arXiv:0801.0629.
- [15] B. Holdom, *Phys. Lett. B* **166**, 196 (1986).
- [16] W. M. Yao et al. [Particle Data Group], *J. Phys. G* **33**, 1 (2006).
- [17] J. Alcaraz et al. [ALEPH Collaboration], arXiv:hep-ex/0612034.
- [18] M. E. Peskin and J. D. Wells, *Phys. Rev. D* **64**, 093003 (2001) [arXiv:hep-ph/0101342].
- [19] A. Djouadi, J. Kalinowski and M. Spira, *Comput. Phys. Commun.* **108**, 56 (1998) [arXiv:hep-ph/9704448]; Program can be found at: <http://people.web.psi.ch/spira/proglist.html>.
- [20] M. Spira, arXiv:hep-ph/9510347. Program can also be found at <http://people.web.psi.ch/spira/proglist.html>.
- [21] A. Djouadi, arXiv:hep-ph/0503172.
- [22] ATLAS Technical Design Report, Vol. 2, CERN/LHCC/99-14 (1999), secs. 19.2.5 & 19.2.9.
- [23] T. Stelzer and W. F. Long, *Comput. Phys. Commun.* **81**, 357 (1994) [arXiv:hep-ph/9401258]. Program can be found at <http://madgraph.phys.uclac.be/index.html>.
- [24] F. Maltoni and T. Stelzer, *JHEP* **0302**, 027 (2003) [arXiv:hep-ph/0208156]. Program can also be found at <http://madgraph.phys.uclac.be/index.html>.
- [25] J. Pumplin, A. Belyaev, J. Huston, D. Stump and W. K. Tung, *JHEP* **0602**, 032 (2006) [arXiv:hep-ph/0512167].
- [26] D0 Collaboration, Note 5345-CONF (March 9, 2007); CDF Collaboration, Note 8775 (5 April 2007).
- [27] A third renormalizable operator involves a SM gauge singlet fermion N with the Yukawa interaction $N_L H$ related to neutrino mass generation (note however that N carries lepton number). We will not discuss this further in this work since our discussion here is largely independent of the presence of such an interaction.